Wirelessly Programmable Class-E GaN-Based 13.56 MHz Transmitter for Wireless Power Transfer

Leandro Díaz, Martín Sivolella, Pablo Pérez-Nicoli, and Fernando Silveira
Instituto de Ingeniería Eléctrica, Facultad de Ingeniería, Universidad de la República. Montevideo, Uruguay.
leandrod@fing.edu.uy; cmsivolella@gmail.com; pablop@fing.edu.uy; silveira@fing.edu.uy

***Abstract*—This paper presents the complete design and implementation of a class-E Power Amplifier (PA) aimed to drive the transmitter coil in a centimeter-range wireless power link at 13.56 MHz. This kind of systems are prone to variations in the transmission distance, orientation, and could be affected by the presence of foreign conductive or ferromagnetic objects. These variations could change the class-E PA load impedance and/or the power delivered to the receiver (Rx). Therefore, the proposed Class-E PA is able to: 1) control its output current in closed-loop to compensate for changes in its load, 2) protect itself against large changes in its load that could strongly affect the operating point increasing power dissipation, and 3) adjust its output current to the value requested by the Rx via Bluetooth Low Energy (BLE). Hence, this paper contributes by presenting not only the design of a comprehensive class-E PA transmitter from a system-level perspective but also addressing various practical aspects essential for actual implementation. Measurement results of the implemented prototype validate the proposed system architecture and its design.**

***Index Terms*—Class-E power amplifier, wireless power transfer (WPT), Active implantable medical devices (AIMDs)**

I. Introduction

Wireless Power Transfer (WPT) has proven to be a useful technology to recharge wearable and Active Implantable Medical Devices (AIMDs) [2]–[4]. Most commercially available charging pads achieve a transfer distance up to a few centimeters, requiring the user to lay the charger on his/her clothes, which limits his/her activity during the charging process. If the WPT link were capable of reaching greater transmission distances, a more comfortable, non-invasive, and even user-imperceptible recharging scheme could be implemented [5], like the one depicted in Fig. 1. Additionally, it would allow recharging implants that are placed deeper inside the body, acting closer to the target organ. In this paper, we focus on the design of the Class-E Power Amplifier (PA) that drives the transmitter (Tx) coil in several centimeter range WPT links, Fig. 1. The selected class-E PA topology is widely used in WPT applications as it achieves high efficiency, preventing temperature elevation within the transmitter.

The operating frequency affects many aspects of the inductive link design. In this work, we set the carrier frequency within the Industrial, Scientific and Medical band, at 13.56 MHz. This, on one hand, eases electromagnetic compatibility requirements, e.g. no restriction on in-band power, only on harmonics. On the other hand, it allows the implementation of light and small receiver coils which is a fundamental aspect due to the size constraints imposed by the target application.

The authors would like to thank Sim4Life by ZMT [1] for providing the simulation software and CSIC Universidad de la República and ANII, Uruguay, for the financial support.

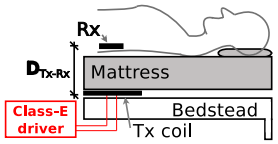

Fig. 1. Designed Class-E PA for centimeter-range WPT.

In this scenario, to maintain both good efficiency and delivered power to the load while bearing with misalignment, the Tx coil requires a large area, i.e., a diameter similar to the target distance [5]. The Tx coil design is out-of-the-scope of this work, and it was designed following the design guidelines presented in [5], leading to a: one-turn, 40 cm diameter Tx coil, with a measured self-inductance of $L_{\text{Tx}} = 1.1\ \mu\text{H}$ and an Equivalent Series Resistance (ESR) of $R_{\text{Tx}} = 1.3\ \Omega$ (at 13.56 MHz). This system could be altered by conductive or ferromagnetic objects, which could modify its load impedance, L_{Tx} and R_{Tx}, and/or the power that is delivered to the Rx. Because of that, the Class-E PA proposed in this paper includes: 1) A closed-loop control to hold the desired Tx output current without being affected by changes in its load. 2) Different protections, Sec. II-D, in order to bear large changes in its load which would strongly affect the operating point, increasing power dissipation. 3) The possibility of adjusting its output current to a value requested by the Rx via Bluetooth Low Energy (BLE). The peak output current is configurable up to a maximum of 2 A, which meets the Specific Absorption Rate (SAR) limits as will be demonstrated through simulations using Sim4Life simulation software [1]. This level of output current (2 A) is adequate for transferring power in the milliwatt range ($\approx$ 5 mW) over tens of centimeters ($\approx$ 30 cm) [5], [6]. A power level in this range is sufficient for various low-power applications [7], and although it is considerably lower than the power transmitted in links where the charger relies on the patient's skin, it offers the advantage of not requiring specific actions from the user, allowing it to operate imperceptibly. Therefore, the contribution of this paper lies in presenting not only the design from a system-level perspective of a complete class-E PA transmitter, but also addressing diverse practical aspects essential for actual implementation.

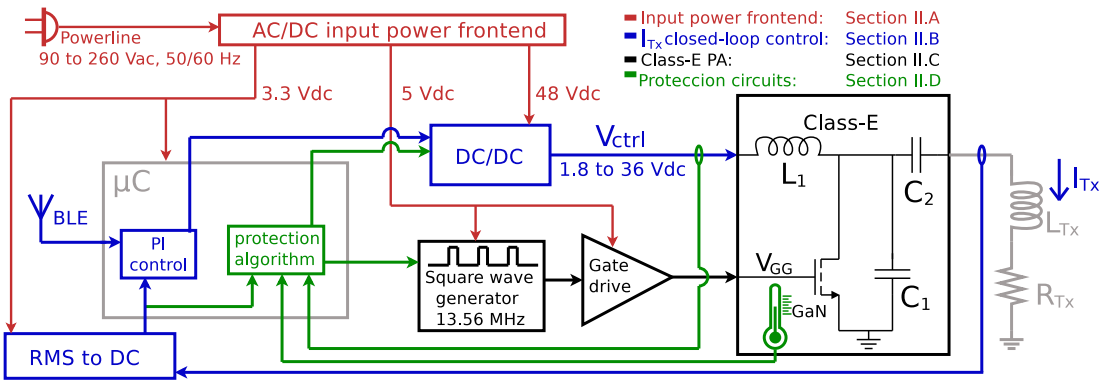

Fig. 2. Block diagram of the proposed transmitter.

This article is organized as follows: First, the proposed architecture and its design procedure is presented in Sec. II. Then, measurement results of the implemented prototype are presented in Sec. III, followed by the main conclusions.

II. Proposed Transmitter

The block diagram of the proposed transmitter is shown in Fig. 2. The following is a brief description of each of the four subsystems that make up the transmitter; a more detailed discussion of each module will be presented in the following subsections:

- RED - Input power frontend, Sec. II-A: Transforms the input electrical power from the powerline into the dc voltage levels required by the other subsystems.
- BLUE - Output current closed-loop control, Sec. II-B: Receives the target amplitude for the output current via BLE, I_{target}, and controls the output current, I_{Tx}, in a closed-loop.
- BLACK - Class-E PA, Sec. II-C: Generates the ac output current, I_{Tx}, with the desired frequency and amplitude.
- GREEN - Protection circuits, Sec. II-D: Monitors system parameters, such as temperature, currents, and voltages, to ensure that the system operates within maximum ratings.

A. Input power frontend

This subsystem is responsible for adapting the input voltage to those required to supply the different circuits that make up the system. Due to the diversity of circuits, it is not possible to use a single voltage level to supply all of them, instead three voltage levels are required: 48 Vdc, 5 Vdc, and 3.3 Vdc.

A block diagram of the Input Power Frontend is depicted in Fig. 3. The input ac voltage from the powerline is connected to an ac/dc converter, which generates an output voltage of 48 Vdc. A fuse and a varistor were included to protect the system against short circuits, overload, and input voltage transients. The 5 Vdc level is obtained from the 48 Vdc voltage level using a synchronous buck dc/dc converter. Finally, the 3.3 Vdc is obtained from the 5 Vdc level using an low-dropout (LDO) linear regulator. This cascade topology, and the converters' architectures, were selected to maximize efficiency while preserving the required power integrity.

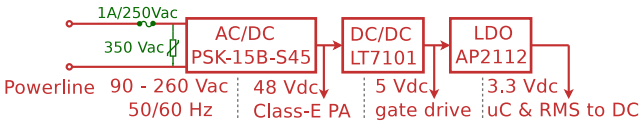

Fig. 3. Block diagram of the Input Power Frontend.

B. Output current closed-loop control

As discussed in Sec. I, the target inductive link is prone to variations during operation. To ensure that the output current, I_{Tx}, matches the target value received via BLE over the whole operation time, a control mechanism is needed.

The proposed architecture for controlling the transmitter's output current, I_{Tx}, is detailed in Fig. 4. The output current of a Class-E PA can be approximated as linearly related to its input voltage [8]. Therefore, a dc/dc converter, powered from the Input Power Frontend, is used to adjust the input voltage of the Class-E PA, thus controlling its output current. The selected dc/dc converter uses a resistor divider to regulate its output voltage in a closed-loop, and it includes all the protections commonly found in buck topology integrated regulators, such as overcurrent protection, thermal shutdown, soft start and light load management. The resistor divider was implemented using a digital potentiometer, enabling digital control of the Class-E PA input voltage and thus controlling its output current to meet the receiver requests.

The output current of a Class-E PA, I_{Tx}, strongly depends on its load, which is in this case the Tx coil, modelled by L_{Tx} and R_{Tx}. Due to the aforementioned expected variations in L_{Tx} and R_{Tx}, imposing the input voltage of the Class-E PA in an open-loop scheme is not enough to maintain its output current at the target value. Therefore, a closed-loop control mechanism was implemented, which senses the output current and adjusts the digital potentiometer accordingly, as depicted in Fig. 4. The sensing loop is composed of a 1:10 transformer, an RMS-to-dc converter, a Low Pass Filter (LPF), and an Analog to Digital Converter (ADC) provided by the microcontroller used. The LPF filters the interference and noise that would otherwise reach the ADC input and also sets the dominant pole of the control loop, ensuring the loop stability. Finally, a Proportional Integral (PI) control algorithm, implemented

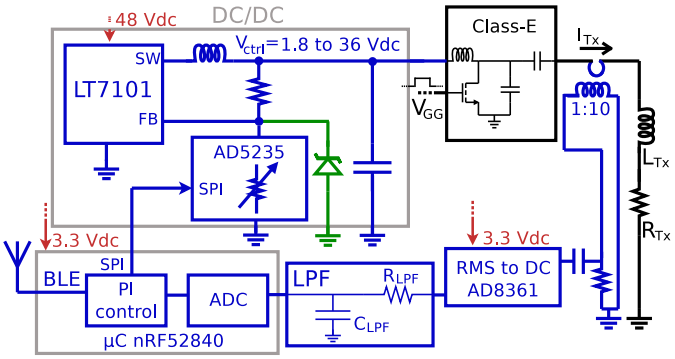

Fig. 4. Proposed closed-loop control for the transmitter output current.

in the microcontroler, compares the measured current value against the target value received by BLE in order to control the digital potentiometer. The PI control algorithm was chosen due to its simplicity, ease of implementation, and it proved to be enough for this application while exhibiting good stability (margin of 81°).

C. Class-E power amplifier

The class-E PA with zero voltage switching (ZVS) and zero voltage derivative switching (ZVDS) can be designed following the guidelines outlined in the reference book published by Kazimierczuk et al. [8]. The design result values are shown in Table I, where D is the duty cycle of the transistor switching signal and the other parameters (components, currents and voltages) are specified in Fig. 2.

A gallium nitride transistor (GaNSystem GS66506T) was selected as it allows for high current, high voltage breakdown, and high switching frequency. This transistor has a low drain–source on-resistance of 67 mΩ, can drive up to 22.5 A continuous drain current, and tolerate a drain-source voltage up to 650 V, meeting the needs of this application. The parasitic drain-source capacitance depends on the drain-source voltage, and it is not easy to deduce an equivalent linear shunt capacitance theoretically [9], [10]. Based on LTspice simulations using the transistor spice model provided by the manufacturer, an equivalent linear shunt capacitance of 330 pF was numerically deduced at maximum output current, $I_{\text{Tx}} = 2$ A. Therefore, this parasitic capacitance should be deducted from the design value obtained for C_1, Table I, $C_1 = 588$ pF-330 pF. This parasitic capacitance approximation, the tolerance of the components used, along with other parasitic capacitances and inductances that were neglected in the analysis such as the gate-drain capacitance [10]–[12], the 1:10 current measurement transformer, and the PCB parasitic capacitance, make it necessary to tune the amplifier (C_1 and C_2) to achieve the ZVS and ZVDS conditions, which is detailed in the next Sec. II-C1.

1) Class-E PA tuning procedure: The tuning procedure described in [13] was followed. Figure 5 illustrates how the "trough" [13] of the waveform is affected by C_1 and C_2. Although L_{Tx} and R_{Tx} also affect the waveform, those values are imposed by the application, thus, in this work,

TABLE I
DESIGN RESULT VALUES FOR CLASS-E PA.

Input/Output	$V_{\text{ctrl}} = [1.8, 36]$ V	$I_{\text{Tx}} = [0.1, 2]$ A
Switching signal	$f = 13.56$ MHz	$D = 0.11$
Load (Tx coil)	$L_{\text{Tx}} = 1.1$ µH	$R_{\text{Tx}} = 1.3$ Ω
Class-E	$C_1 = 588$ pF $C_2 = 155$ pF	$L_1 = 47$ µH

only C_1 and C_2 were manually adjusted to tune the PA. The tuning procedure was performed at maximum output power, $I_{\text{Tx}} = 2$ A, to ensure high efficiency at the most critical operating point.

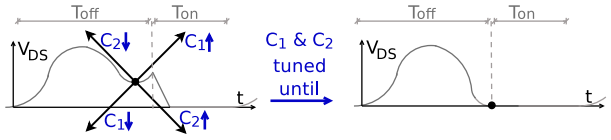

Fig. 5. Impact of C_1 and C_2 on the ZVS and ZDVS [13], used to tune the Class-E PA.

2) Class-E PA switching signal generation: To conclude the class-E PA implementation, the square wave generator and the gate driver that generates the switching signal are presented in this section, Fig. 6. The square wave generator is based on the solution implemented in [14], where the rectangular wave generated by a 13.56 MHz (±50 ppm) oscillator is converted to a rather triangular wave by an R-C low-pass filter, and compared to a dc set point voltage. The dc set point voltage is controlled by means of a variable resistive divider, thus allowing fine-tuning of the duty cycle to achieve the desired value. Then, the signal is power amplified by the gate drive circuit.

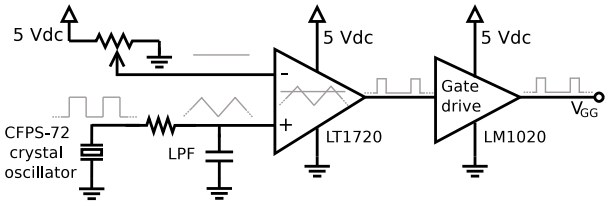

Fig. 6. Schematic circuit of the square wave generator.

D. Protection circuits

As discussed in Sec. I, the model of the Tx coil, L_{Tx} and R_{Tx}, could change during operation especially due to the presence of conductive or ferromagnetic foreign objects. If that happens, the operating point of the class-E power amplifier is affected, strongly reducing its efficiency as the ZVS and ZDVS are no longer satisfied. This scenario, as well as other faults that could occur, may generate overvoltages, overcurrents, and/or over temperatures, damaging the circuit. Therefore, the protections described below, and depicted in green color in the previous figures, were included. In all the cases, when an overvoltage, overcurrent, and/or over temperature is detected, the class-E PA and its gate drive circuit are turned off by disabling the dc/dc converters that feed them, i.e., grounding the RUN pin of the dc/dc converters (LT7101) shown in Fig. 4.

Fig. 7. Implemented prototype (231 mm x 99 mm).

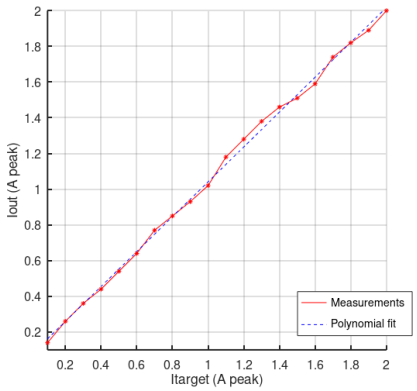

Fig. 8. Target current and steady state output current.

Class-E PA, output overcurrent: The class-E output current is monitored by the microprocessor and regulated in closed-loop as detailed in Sec. II-B. Therefore, if the microprocessor measured current exceeds the preset value by more than 10%, the protection is activated.

Class-E PA, Power transistor over temperature: The TC77 digital temperature sensor is used to monitor the class-E power transistor, reporting its temperature to the microprocessor via SPI. The maximum operating junction temperature is $150°$C. Considering that the temperature is being measured in the ground thermal pad, where the temperature is lower than in the junction, and including a safety margin, the threshold that triggers the protection was set at $80°$C.

Adjustable dc/dc (LT7101, Fig. 4), feedback pin overvoltage: The discrete variation between values of the digital potentiometer (AD5235), Fig. 4, could cause an overvoltage in the feedback pin of the LT7101 dc/dc regulator. Therefore, a 2.7 V zener diode was included as shown in Fig. 4.

Adjustable dc/dc (LT7101, Fig. 4), output overcurrent: A failure in the class-E PA could also generate an overcurrent in the dc/dc that feeds it, which may damage it even before the class-E PA protection acts. Therefore, the ICTRL PIN of the LT7101 was used to limit its output current to a value 46% greater than the current required by the class-E PA at maximum power ($I_{\text{Tx}} = 2\ A$), $1.46 \times 76\ mA = 111\ mA$.

Powerline: A 3.15 A fuse and a 350 V_{rms} varistor were included, Fig. 3, to prevent overcurrents and handle surges respectively.

III. Measurement Result

The implemented prototype is presented in Fig. 7. The measured output current is depicted in Fig. 8, demonstrating that the amplifier is capable of adjusting it within the target range, while showing good linearity. The coefficients of a first-order polynomial fit for the data resulted in 64 mA_{peak} and 0.977 $\frac{A_{peak}}{A_{peak}}$, zero and first-order respectively. The RMSE (Root Mean Squared Error) between the polynomial fit and the data resulted in 26.3 mA_{peak}.

In order to prove that the proposed transmitter meets the SAR limits for general public while driving the target coil, Sim4Life [1] simulations were performed. The simulation

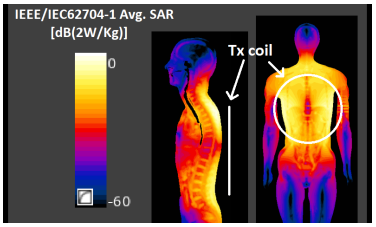

Fig. 9. Sim4Life SAR simulation at maximum output current, $I_{\text{Tx}} = 2\ A$.

results are presented in Fig. 9. This simulation was done at maximum output current, $I_{\text{Tx}} = 2\ A_{peak}$, laying the heterogeneous Duke virtual population model over the Tx coil (3 cm distance due to Tx case), and the SAR was calculated as the average over 1 g of tissue. The maximum simulated SAR was 1.87 W/kg which is lower than the most restrictive (for the head) general public limit, 2 W/kg [15], [16]. The simulated whole body average is 0.026 W/kg which also meets the general public limit of 0.080 W/kg [15].

Accurately measuring efficiency during operation, when the amplifier is loaded with the transmitting coil, is challenging due to the high-intensity magnetic field generated by the system, which couples into the measurement setup. Therefore, the efficiency of the Class E was estimated through simulation, resulting in 95% (including gate drive) at maximum output current ($I_{\text{Tx}} = 2\ A_{peak}$). The whole system efficiency (Class E ouput power divided by the power consumed from the mains) was estimated in measurements, resulting in approximately 75% also at maximum output current.

IV. Conclusion

In this work, the design and implementation of a complete Class-E transmitter for wireless power transfer are presented. The proposed architecture is able to: 1) control its output current in a closed-loop to compensate for changes in the load L_{Tx} and R_{Tx}, 2) protect itself against large changes in its load that could strongly affect the operating point increasing power dissipation, for which different protections were included, and 3) adjust its output current to the value requested by the Rx via BLE. The design was validated through measurement results of the fabricated prototype.

REFERENCES

[1] Sim4Life by ZMT. [Online]. Available: www.zurichmedtech.com

[2] T. Sun, X. Xie, and Z. Wang, *Wireless power transfer for medical microsystems*. Springer, 2013.

[3] D. Haci, Y. Liu, S. S. Ghoreishizadeh, and T. G. Constandinou, "Key considerations for power management in active implantable medical devices," in *2020 IEEE 11th Latin American Symposium on Circuits & Systems (LASCAS)*. IEEE, 2020, pp. 1–4.

[4] P. Pérez-Nicoli, F. Silveira, and M. Ghovanloo, *Inductive Links for Wireless Power Transfer*. Springer, 2021.

[5] P. Pérez-Nicoli, M. Sivolella, N. Gammarano, and F. Silveira, "Limits for increasing the WPT distance in AIMDs," in *2020 XXXIIIrd General Assembly and Scientific Symposium of the International Union of Radio Science*. IEEE, 2020, pp. 1–4.

[6] ——, "Patient imperceptible wpt for wearable/implantable medical devices," in *2021 XXXIVth General Assembly and Scientific Symposium of the International Union of Radio Science (URSI GASS)*. IEEE, 2021, pp. 1–4.

[7] A. P. Chandrakasan, N. Verma, and D. C. Daly, "Ultralow-power electronics for biomedical applications," *Annu. Rev. Biomed. Eng.*, vol. 10, pp. 247–274, 2008.

[8] D. C. Marian K. Kazimierczuk, *Resonant Power Converters*, 2nd ed. New York: Wiley, 2011.

[9] T. Suetsugu and M. K. Kazimierczuk, "Comparison of class-E amplifier with nonlinear and linear shunt capacitance," *IEEE Transactions on Circuits and Systems I: Fundamental Theory and Applications*, vol. 50, no. 8, pp. 1089–1097, 2003.

[10] M. Hayati, A. Lotfi, M. K. Kazimierczuk, and H. Sekiya, "Analysis and design of class-E power amplifier with MOSFET parasitic linear and nonlinear capacitances at any duty ratio," *IEEE Transactions on Power Electronics*, vol. 28, no. 11, pp. 5222–5232, 2013.

[11] X. Wei, H. Sekiya, S. Kuroiwa, T. Suetsugu, and M. K. Kazimierczuk, "Effect of MOSFET gate-to-drain parasitic capacitance on class-E power amplifier," in *Proceedings of 2010 IEEE International Symposium on Circuits and Systems*. IEEE, 2010, pp. 3200–3203.

[12] ——, "Design of class-E amplifier with MOSFET linear gate-to-drain and nonlinear drain-to-source capacitances," *IEEE Transactions on Circuits and Systems I: Regular Papers*, vol. 58, no. 10, pp. 2556–2565, 2011.

[13] N. O. Sokal and I. L. Fellow, "Class-E high-efficiency RF/microwave power amplifiers: Principles of operation, design procedures, and experimental verification," in analog circuit design: Scalable analog circuit design," *High-Speed D/A Converters, RF Amplifiers, J. H. Huijsing et al., Eds. Dordrecht, The Netherlands: Kluwer*, pp. 269–301.

[14] S. Stoecklin, T. Volk, A. Yousaf, and L. Reindl, "A programmable and self-adjusting class E amplifier for efficient wireless powering of biomedical implants," in *2015 37th Annual International Conference of the IEEE Engineering in Medicine and Biology Society (EMBC)*, 2015, pp. 3193–3196.

[15] ICNIRP, "Guidelines for limiting exposure to electromagnetic fields (100 kHz to 300 GHz)," International Commission on Non-Ionizing Radiation Protection, ICNIRP, Standard, Apr. 2020.

[16] S. Cetin and Y. E. Demirci, "High-efficiency LC-S compensated wireless power transfer charging converter for implantable pacemakers," *International Journal of Circuit Theory and Applications*, vol. 50, no. 1, pp. 122–134, 2022.